Eulerian diagnostics for Lagrangian chaos in three-dimensional Navier-Stokes flows

A. N. Yannacopoulos,[1] I. Mezić,[2] G. Rowlands,[1] and G. P. King[3]
[1]*Department of Physics, University of Warwick, Coventry CV4 7AL, United Kingdom*
[2]*Department of Mechanical and Environmental Engineering, University of California, Santa Barbara, California 93106-5070*
[3]*Fluid Dynamics Research Centre, Department of Engineering, University of Warwick, Coventry CV4 7AL, United Kingdom*
(Received 18 April 1997; revised manuscript received 12 September 1997)

Based on symmetry considerations, Eulerian quantities are defined which can serve as diagnostics for the regions of the flow where Lagrangian chaos is possible in a three-dimensional Navier-Stokes flow. The applicability of the diagnostics is tested in two model flows which are perturbative solutions of the three-dimensional Navier-Stokes equation: the eccentric Taylor vortex and the (concentric) wavy Taylor vortex. [S1063-651X(98)01101-5]

PACS number(s): 47.15.−x

I. INTRODUCTION

It is well known by now that the motion of a passive tracer in a laminar fluid flow can be very complicated, giving rise to Lagrangian chaos. Such behavior might appear in the case of a two-dimensional flow with a periodic time dependence or a fully three-dimensional flow. Whereas the case of two-dimensional time-dependent flows is relatively well understood (see, for instance, Refs. [1–3]), a smaller number of studies has been devoted to similar phenomena in three-dimensional flows [4–12]. Furthermore, the three-dimensional studies were based on kinematic models which are not solutions of the Navier-Stokes equations, and therefore can be expected to lack the essential physical features of the problem. The exception are a few recent studies [13–15] in which particle paths in perturbative solutions of the Navier-Stokes equations have been studied in some detail.

The aim of this paper is to study the physics of chaotic advection in a three-dimensional solution of the Navier-Stokes equation. It was pointed out in Ref. [10] that viscous effects determine the chaoticity of three-dimensional Navier-Stokes flows away from the boundaries, where the motion can be considered almost dissipation free. As Arnold [16] observed, steady bounded analytic Euler flows for which vorticity and velocity are not parallel, bounded by analytic surfaces in three-dimensional Euclidian space, admit a nontrivial symmetry generated by vorticity and thus are integrable. This integrability can be broken by viscous effects. In fact, as we show below, via a simple argument, that the above integrability theorem of Arnold can be extended to include the flows that are viscous but have a flexion potential (i.e., the curl of vorticity is a potential vector field; this includes flexion-free fields for which the curl of vorticity is zero [17]). A related work was carried out by Kozlov in Ref. [18], where he proved that viscous flows typically do not possess integrals of motion. However, the geometry of the boundaries often impose volume-preserving symmetries that preserve integrability even though the dynamical symmetry imposed by the Euler equations is broken. Such symmetries need to be accounted for in any integrability considerations. For example, Couette flow is viscous but rotationally symmetric, and thus integrable. In this paper we introduce Eulerian diagnostics—quantities which are local functions of the velocity and its gradients—which highlight the regions where Lagrangian chaos is possible. This is done following a symmetry approach suggested by the work in Refs. [10,11] (for an extension, see Ref. [19]). The symmetries we use are geometric (related to the boundary conditions or the geometry of the container) and dynamical symmetries—those related to the physics of the flow, and in particular to the dynamics of the Navier-Stokes equation. We show that the location of chaotic zones in three-dimensional steady flows is related to zones where some of the symmetries of the problem are broken. We propose measures for symmetry breaking which are Eulerian quantities. Our results are valid for steady flows, or flows which are steady in a rotating frame. They are tested on analytical perturbative solutions for the flow between concentric cylinders and eccentric cylinders (with small eccentricity) given by Davey, DiPrima, and Stuart [20] and DiPrima and Stuart [21], respectively.

It is important to note that the results presented here can be justified rigorously in perturbative situations: the positivity of the proposed diagnostic in certain regions of the physical space implies, by Melnikov-type calculation, chaos. Here the unperturbed flow is an Euler flow, and its perturbation is provided by viscous terms. In this context, the integrability of the unperturbed, Euler flow is assumed. Thus, the case of Arnold-Beltrani-Childress (ABC) flows [22,23] is excluded from our considerations. Despite their popularity as toy models for chaotic advection in three-dimensional steady fluid flows, we believe ABC flows are, due to the relationship between velocity and vorticity, exceptional in the class of Euler flows in a three-dimensional Euclidean space.

II. DEFINITION OF EULERIAN DIAGNOSTICS

In this section we define Eulerian diagnostics for the regions of the flow where chaotic streamlines might appear. A volume-preserving symmetry imposes constraints on the dynamics of three-dimensional, steady incompressible flows in the form of a constant of the motion [11,16,24]. This means that the orbits are constrained to lie on a two-dimensional surface, and thus the dynamics are reducible to those of a two-dimensional system for which the orbits will have to follow regular dynamics. For a detailed account of the effect

of symmetries in three-dimensional volume preserving flows, see Refs. [10,11,24].

A. Geometrical symmetries

Geometric symmetries are dictated by the geometry of the flow. An example of such a symmetry is the azimuthal symmetry in the Taylor vortex between concentric rotating cylinders. Such a geometric symmetry is broken when the velocity field becomes dependent on the azimuthal direction. For the particular case of the Taylor vortex this is achieved either by making the system eccentric or by the onset of a wave. In both of these cases chaotic streamlines can appear [13–15].

B. Dynamical symmetries

Dynamical symmetries are in general more difficult to spot than the geometrical ones. They are associated with the physics of the flow. The dynamical symmetry that we consider is associated with the steady Navier-Stokes equation for a fluid of constant unit density:

$$\boldsymbol{\omega}\times\mathbf{v}+\tfrac{1}{2}\nabla\mathbf{v}^2=-\nabla P+\nu\nabla\times\boldsymbol{\omega}, \tag{2.1}$$

where $\boldsymbol{\omega}$ is the vorticity, $\boldsymbol{\omega}\times\mathbf{v}$ is the Lamb vector, P is the pressure and the term $\nabla\times\boldsymbol{\omega}$ is the *flexion field* [17]. The familiar Bernoulli function associated with Euler flows and defined by

$$B=\frac{\mathbf{v}^2}{2}+P \tag{2.2}$$

changes along a trajectory according to

$$\frac{dB}{dt}=\nu(\nabla\times\boldsymbol{\omega})\cdot\mathbf{v}. \tag{2.3}$$

It is clear that if the flexion field vanishes or is always perpendicular to the velocity then B is a constant of the motion. This implies integrability if B is not a constant everywhere. For flows in which $\nu\nabla\times\boldsymbol{\omega}=0$, the only case in which chaotic motion is possible is that of Beltrami flows $\mathbf{v}=c\boldsymbol{\omega}$ for which the constant of proportionality c is independent of space. When $\nabla\times\boldsymbol{\omega}=0$, the only element of this set of vector fields is that with zero velocity everywhere. If $\nu=0$ (the case of a Euler flow) flows with $\mathbf{v}=c\boldsymbol{\omega}$ are the only ones with the possibility of chaotic motion. We make a distinction between flows with $\nabla\times\boldsymbol{\omega}=0$, and $\nu=0$ because, although they solve the same equation, they do not satisfy the same boundary conditions. In these cases the motion is restricted to Lamb surfaces $B=\text{const}$ [17]. This was observed by Arnold [16], who also investigated the topological structure of these surfaces, and proved that they were cylinders or tori in the case of an analytical velocity field bounded by an analytic surface. In Refs. [10,11,24] it was proven that such a symmetry implies that coordinates can be constructed such that the velocity field is a Hamiltonian system in two of the variables, and the dynamics of the third variable depends only on the dynamics of the Hamiltonian part.

The term $\nu(\nabla\times\boldsymbol{\omega})$ clearly determines the importance of dissipative effects in the flow. A quantity that measures the relative importance of inertial and dissipative effects at each point in the flow is the local Reynolds number defined as the ratio of the magnitude of the inertial term over the magnitude of the dissipation

$$\mathrm{Re}_l=\frac{|\mathbf{v}\cdot\nabla\mathbf{v}|}{|\nu\nabla\times\boldsymbol{\omega}|}. \tag{2.4}$$

In regions where this number is large, inertial effects dominate dissipative effects, and regular motion is expected. In the regions where this number is small, Lagrangian chaos is likely to occur. We will see that Re_l is too crude a diagnostic for Lagrangian chaos. We thus turn to symmetry considerations.

Taking the curl of Eq. (2.1) we obtain

$$\boldsymbol{\omega}\cdot\nabla\mathbf{v}-\mathbf{v}\cdot\nabla\boldsymbol{\omega}=\nu\nabla\times(\nabla\times\boldsymbol{\omega}). \tag{2.5}$$

The left-hand side is the so-called Lie bracket of the velocity and vorticity field. When the Lie bracket vanishes—a particular instance of which is when the flexion field is zero—the two vector fields commute, and the integrability of both is implied if they are nowhere parallel [16,24]. Thus, a constant of motion exists if $\nu\nabla\times\nabla\times\boldsymbol{\omega}=0$, i.e., $\nabla\times\boldsymbol{\omega}=-\nabla\sigma$ for some smooth function σ called the *flexion potential* [17]. The constant of motion is given by

$$B=\frac{\mathbf{v}^2}{2}+P+\nu\sigma.$$

Note that creeping flows in Stokes approximations satisfy $\nabla\times\nabla\times\boldsymbol{\omega}=0$. But it is not true in general that Stokes flows are integrable. Indeed, consistent with the Stokes approximation we could neglect $\mathbf{v}^2/2$ in the expression for B, and expect that the integral of motion is $B=P+\nu\sigma$. But the function σ for Stokes flows satisfies $\nabla P+\nu\nabla\sigma=0$. Thus $\sigma=-P/\nu+C$, where C is an arbitrary constant, and the integral of motion becomes trivial.

C. A Eulerian diagnostic for chaotic advection

Very often there is an interplay of more than one symmetry in a system. One of the symmetries can break down, but another persists and preserves integrability. An example is provided by the transition from Couette flow to Taylor vortex flow. The Couette flow possesses the dynamical symmetry as it is flexion-free ($\nabla\times\boldsymbol{\omega}=\mathbf{0}$), geometric translational symmetry along the z axis, and the geometric azimuthal symmetry, all of which are volume preserving. The first two of these are broken with the onset of Taylor vortices, but the geometric azimuthal symmetry persists, ensuring integrability. Another example is the eccentric Couette flow considered as a perturbation of the concentric Couette flow. The dynamical symmetry in the eccentric flow is broken, because with the onset of eccentricity the flexion field becomes nonzero. The geometric azimuthal symmetry is also broken, but the translational invariance in the direction of z is not broken and preserves integrability. In order that chaotic advection is possible, all of the symmetries of the unperturbed problem need to be broken. Generally, it is not easy to identify all of the symmetries. But in the perturbative setting it is natural to search among the symmetries of the unperturbed problem.

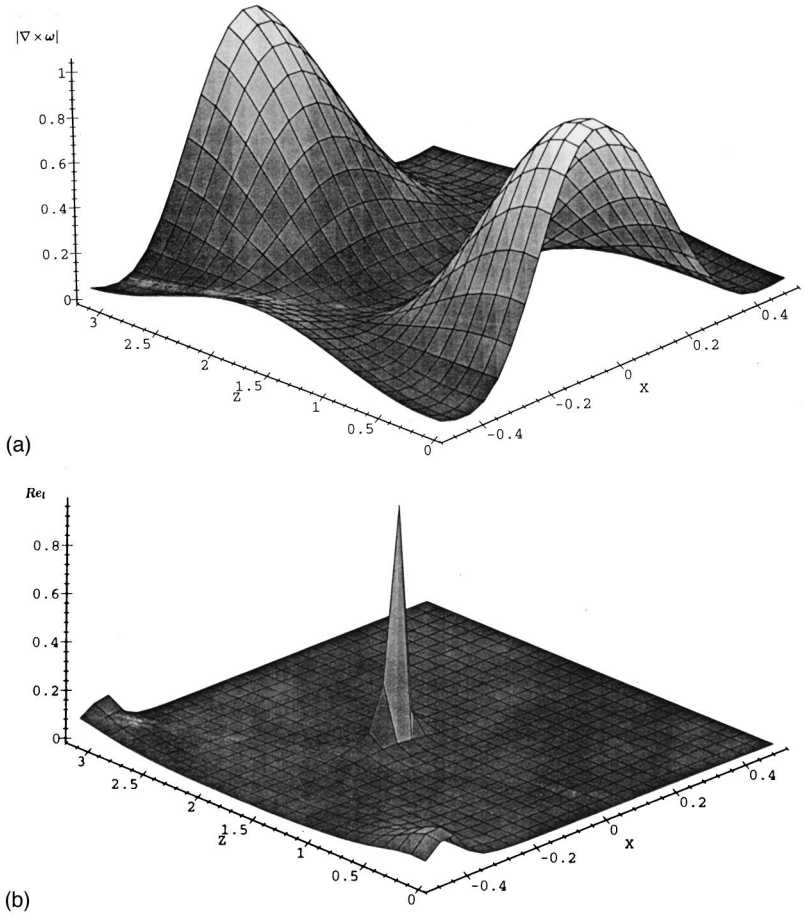

FIG. 1. (a) The flexion field magnitude $|\nabla \times \boldsymbol{\omega}|$, and (b) the local Reynolds number Re_l for the wavy Taylor vortex at $\psi=0$ in the comoving frame of the wave. These quantities have been scaled by their maximum values. The outflow boundary is located at $z=0$, and the inflow boundary at $z=\pi$.

For Navier-Stokes flows at high Reynolds numbers the flow can be considered, away from the boundaries, as a small perturbation of an Euler flow. Symmetries arising from the geometry of the container are another natural choice.

Based on the above discussion, we define an Eulerian diagnostic $\mathcal{D}$ which measures the pointwise deviation from the symmetries of the unperturbed problem. A plot of $\mathcal{D}$ as a function of space will show where $\mathcal{D}$ deviates from zero, and hence will highlight the regions where chaotic streamlines and enhanced mixing are expected. Since in our examples the unperturbed problem is concentric or eccentric Couette flow with the above described symmetries, we define

$$\mathcal{D}=(\nabla\times\boldsymbol{\omega})^2\left(\frac{\partial\mathbf{v}}{\partial\theta}\right)^2\left(\frac{\partial\mathbf{v}}{\partial z}\right)^2. \tag{2.6}$$

Let us denote the generator of the azimuthal symmetry group by $\mathbf{w}_\theta=(0,1,0)$ in cylindrical polar coordinates (x,θ,z), and the generator of the axial symmetry by $\mathbf{w}_z=(0,0,1)$. The terms $\partial\mathbf{v}/\partial\theta$ and $\partial\mathbf{v}/\partial z$ are related to Lie brackets of the velocity field with the generator of the geometrical symmetry group by $[(1/r)(\partial\mathbf{v}/\partial\theta)]=[\mathbf{v},\mathbf{w}_\theta]$ and $(\partial\mathbf{v}/\partial z)=[\mathbf{v},\mathbf{w}_z]$. Thus they are zero in the case when $\mathbf{v}$ admits the corresponding symmetry group. For the dynamical symmetry, we choose to measure the deviation from symmetry by

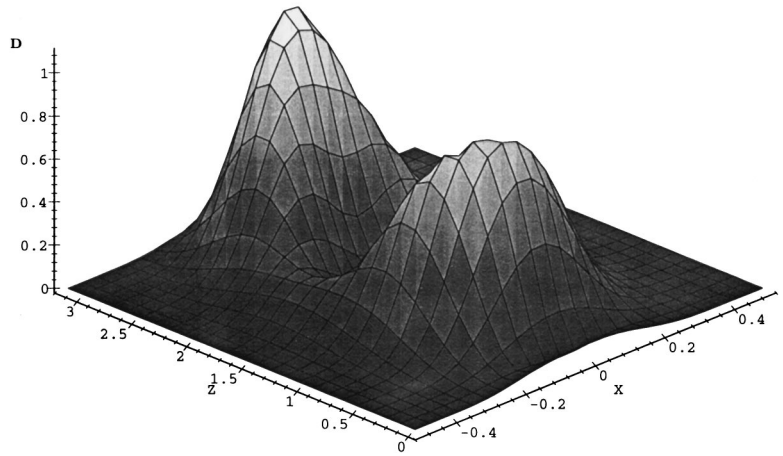

FIG. 2. The Eulerian diagnostic $\mathcal{D}$ for the wavy Taylor vortex at $\psi=0$ in the comoving frame of the wave. $\mathcal{D}$ is scaled by its maximum value.

$(\nabla\times\boldsymbol{\omega})$, and not the Lie bracket of velocity and vorticity $\nu(\nabla\times\nabla\times\boldsymbol{\omega})$. This is primarily because of the fact discussed above that the latter term is zero for a possibly nonintegrable Stokes flow. An additional reason is based on the perturbative nature of the cases we treat: as was shown above, $\nu\nabla\times\boldsymbol{\omega}$ is the term that is responsible for deviations from constancy of the Bernoulli integral.

III. APPLICATION OF THE DIAGNOSTIC IN TWO EXAMPLES

In this section we apply the diagnostic tools we proposed in Sec. II to two examples of a Navier-Stokes flow. Both of these examples are perturbations of the flexion-free Couette flow. The first one is the wavy vortex mode solution obtained by Davey, DiPrima, and Stuart [20], for which Lagrangian properties were studied in Refs. [14,15]. In the second example the perturbation is due to eccentricity. This solution was obtained by DiPrima and Stuart [21], and its Lagrangian properties were studied in Ref. [13].

A. Concentric case

Consider the fluid flow between two infinitely long concentric cylinders. Let

$$\Omega_0=\frac{\Omega_1+\Omega_2}{2},\quad \alpha=2\left(\frac{1-\mu}{1+\mu}\right),\quad \mu=\frac{\Omega_2}{\Omega_1},\qquad (3.1)$$

where Ω_1 denotes the angular velocity of the inner cylinder and Ω_2 the angular velocity of the outer cylinder. The radii of the cylinders are denoted by R_1 and R_2, with $R_2>R_1$. Let

$$R_0=\frac{R_1+R_2}{2},\quad d=R_2-R_1,\quad \delta=\frac{d}{R_0}.\qquad (3.2)$$

The coordinates are defined as

$$R=R_0+xd,\quad Z=zd,\qquad (3.3)$$

with (x,θ,z) cylindrical polar coordinates. The Taylor number T is defined by

$$T=-\frac{4A\Omega_0 d^4}{\nu^2},$$

where A is given by

$$A=\frac{R_2^2\Omega_2-R_1^2\Omega_1}{R_2^2-R_1^2}.$$

The velocity field $\mathbf{v}=(v_x,v_\theta,v_z)$ is given to the first order in the gap parameter δ by

$$\begin{aligned}v_x=&-2\alpha\Omega_0\delta^{3/2}T^{1/2}[A_c(\tau)f_{20}(x)\cos(z)\\&+B_c(\tau)h_{20}(x)\cos(z)e^{im\theta}\\&+B_s(\tau)l_{20}(x)\sin(z)e^{im\theta}+\text{c.c.}],\end{aligned}$$

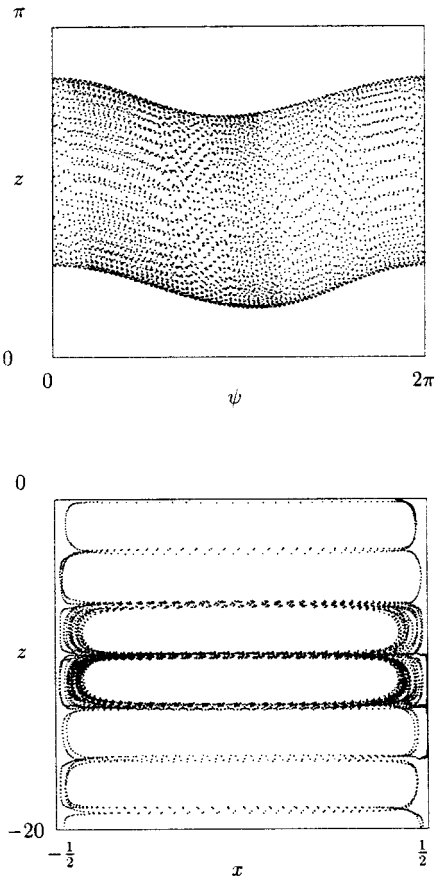

FIG. 3. Particle paths for the wavy Taylor vortex flow. (a) The trajectory of a particle that remains on the surface of a two-dimensional torus centered on the core of a Taylor vortex. (b) The trajectory of a fluid element whose initial position lies outside the torus in (a). The fluid element wanders from vortex to vortex in an irregular manner.

$$\begin{aligned}v_\theta=&\delta\Omega_0 d^{-1}[1-\alpha x+A_c(\tau)f_0(x)\cos(z)\\&+B_c(\tau)h_0(x)\cos(z)e^{im\theta}\\&+B_s(\tau)l_0(x)\sin(z)e^{im\theta}+\text{c.c.}],\end{aligned}$$

$$\begin{aligned}v_z=&-2\alpha\Omega_0\delta^{3/2}T^{1/2}[A_c(\tau)f_{30}(x)\sin(z)\\&+B_c(\tau)h_{30}(x)\sin(z)e^{im\theta}\\&+B_s(\tau)l_{30}(x)\cos(z)e^{im\theta}+\text{c.c.}],\end{aligned}$$

where c.c. denotes complex conjugate.

The functions $f_0,f_{20},f_{30},h_0,h_{20},h_{30},g_0,g_{20}$, and g_{30} are functions of the radial coordinate x, and are given by the solution of boundary value problems. For more details on the boundary value problems these functions have to satisfy, the reader is referred to Refs. [15,20]. The terms proportional to A_c are the contribution of the Taylor vortex, and the terms proportional to B_s are the contribution of the wavy vortex.

1. Wavy vortex flow

In this paper we will consider the following parameter values for the wavy vortex:

$$A_c=0.3442,\quad B_s=0.0336e^{i\omega t},\quad \omega=-5.1380.\qquad (3.4)$$

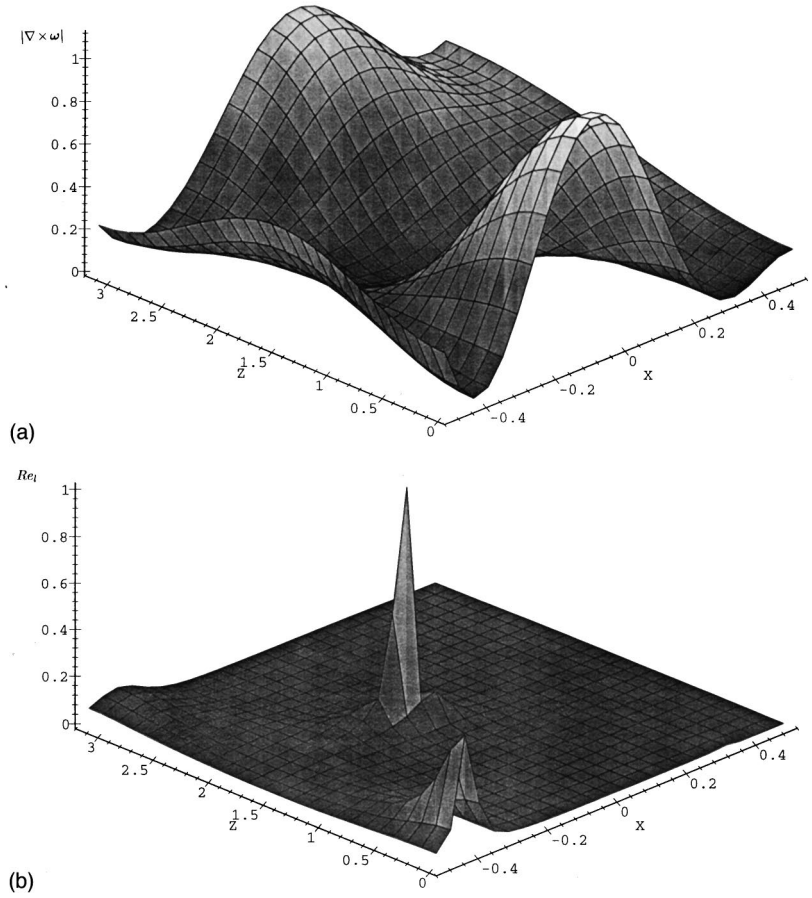

FIG. 4. (a) The flexion field magnitude $|\nabla \times \boldsymbol{\omega}|$, and (b) the local Reynolds number Re_l for the small eccentricity ($\epsilon = 0.1$) Taylor vortex case. The vortex amplitude is $A = 1000$. The quantities are calculated at $\theta = -\pi/2$ and are scaled by their maximum value there. The outflow boundary is located at $z = 0$ and the inflow boundary at $z = \pi$.

The Taylor number has the value $T = 1855$, with $\delta = 0.05$ and $\mu = 0$, in accordance with the values used in Ref. [15]. The wavy vortex is a steady flow in the frame rotating with the wave, and so the dynamical symmetry described above holds. Thus the results shown in Figs. 1–3 are computed in the comoving frame. Note that ψ denotes the azimuthal coordinate in this frame.

In Fig. 1(a) we show the flexion field magnitude $|\nabla \times \boldsymbol{\omega}|$, and in Fig. 1(b) the local Reynolds number Re_l for the wavy Taylor vortex at $\psi = 0$. Note that the vortex inflow boundary is located at $z = \pi$ and the outflow boundary at $z = 0$. The plot of Re_l has a peak in the center of the vortex, showing that the fluid is nearly inviscid there.

In Fig. 2 we show a plot of the Eulerian diagnostic $\mathcal{D}$. Comparing this figure with Fig. 1(a), we see that $\mathcal{D}$ is relatively small near the boundaries compared to $|\nabla \times \boldsymbol{\omega}|$. This is due to the fact that in the perturbed problem the azimuthal symmetry is not heavily broken near the boundaries, and so $\partial \mathbf{v}/\partial \theta$, and hence $\mathcal{D}$, is close to zero there. The same holds for the axial symmetry near the separating surfaces $z = k\pi$, $k = 0, \pm 1, \ldots$. It is easy to see that the total area over which $\mathcal{D}$ is small is considerably larger than the area where the flexion field magnitude is small, thus clearly showing the interaction of the dynamical and geometric symmetries.

Finally we note that on comparing the plot of $\mathcal{D}$ with the particle orbits in the wavy Taylor vortex shown in Fig. 3, we find that the regions where $\mathcal{D}$ attains its minimum value correspond to the regions of (near) integrable streamlines, whereas its peaks correspond to regions where chaotic streamlines occur.

B. Eccentric Taylor vortex

We now apply our diagnostic tool to the eccentric Taylor vortex flow using the asymptotic solution of DiPrima and Stuart [21]. The particle paths for this flow were studied in Ref. [13]. We briefly summarize the flow field, and refer the reader to the above two references for more details. The coordinate system used is a bipolar coordinate system such that x is a scaled radial coordinate (ρ being the original radial coordinate) corresponding to $-\frac{1}{2}$ on the inner cylinder, and to $\frac{1}{2}$ on the outer cylinder, θ is an angular coordinate corresponding to $\theta = 0$ at the large gap and to $\theta = \pi$ at the small gap, and z is a suitably scaled coordinate along the axes of the cylinders. The velocity field is given by

$$v_\rho = \frac{\alpha}{2}\epsilon U(x,\theta) + \frac{1}{\alpha Q}\epsilon^{1/2} u_{\mathrm{TV}}, \tag{3.5}$$

$$v_\theta = \tfrac{1}{2} V(x,\theta) + \epsilon^{1/2} v_{\mathrm{TV}}, \tag{3.6}$$

$$v_\zeta = \frac{1}{\alpha Q}\epsilon^{1/2} w_{\mathrm{TV}}, \tag{3.7}$$

where $U(x,\theta)$ and $V(x,\theta)$ are the contributions of the eccentric Couette flow which clearly has a geometric symmetry with respect to translations along the z axis. The terms with subscripts TV are the Taylor vortex contribution, which are given by

$$u_{\mathrm{TV}} = -B(\theta) f_0(x) \cos(z), \tag{3.8}$$

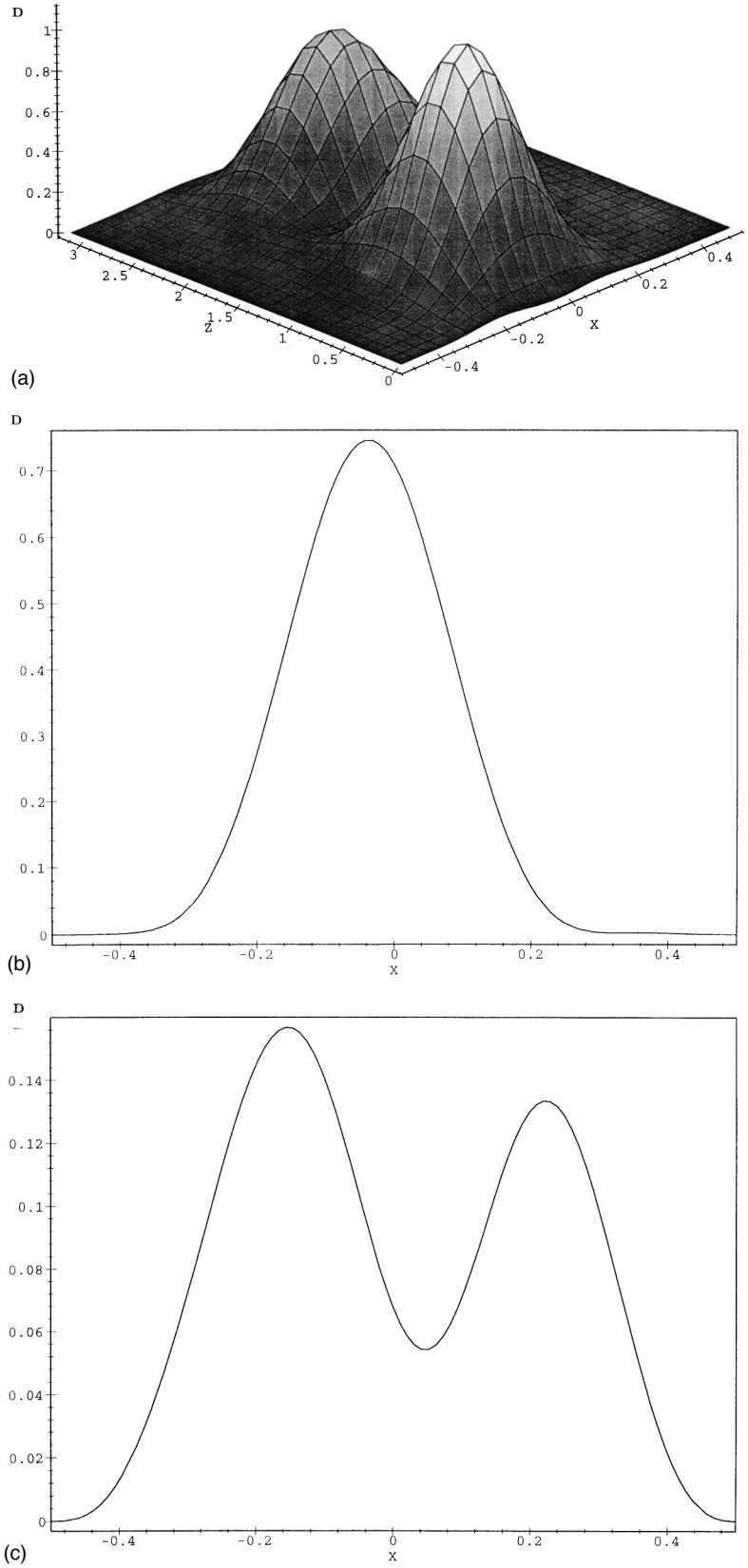

FIG. 5. The Eulerian diagnostic $\mathcal{D}$ at $\theta=-\pi/2$ scaled by its maximum value, for the small eccentricity Taylor vortex case. (a) **D** as a function of x and z. (b) A plot of $\mathcal{D}$ taken at $z=0.5$. (c) A plot of $\mathcal{D}$ taken at $z=1.5$.

$$v_{\mathrm{TV}}=B(\theta)g_0(x)\cos(z), \tag{3.9}$$

$$w_{\mathrm{TV}}=\lambda^{-1}Df_0(x)\sin(z), \tag{3.10}$$

$$B^2(\theta)=A^2\exp\left(\frac{\omega[\sin(\theta)-1]}{k}\right), \tag{3.11}$$

where $\omega=1.122$, and k is obtained by the equality $\alpha=4k^2\epsilon^2$. In the above Q is the velocity of the inner cylinder, the outer is stationary, ϵ is the eccentricity parameter, λ is the axial wave number for the vortex, $\alpha=\delta(1-\epsilon^2)^{1/2}$, where $\delta=[(b-a)/a]$, $a<b$ are the radii of the cylinders, and A is the amplitude of the Taylor vortex. The functions $f_0(x)$

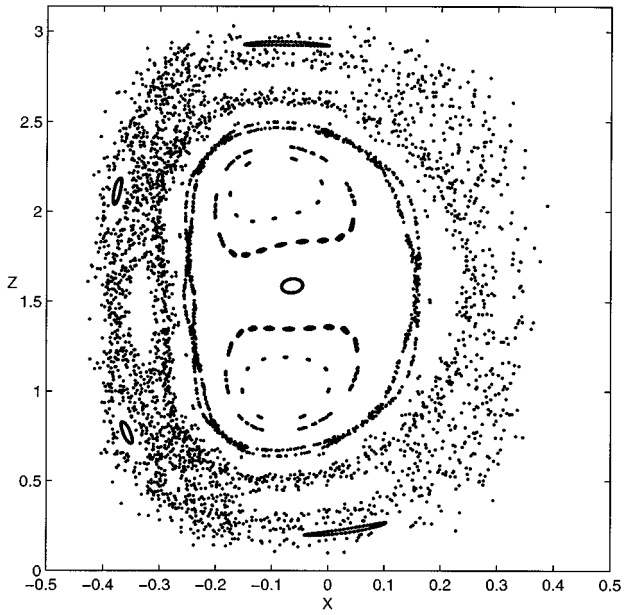

FIG. 6. Surface of section for the small eccentricity Taylor vortex taken at the position of largest gap ($\theta=0$).

and $g_0(x)$ are the solutions of some suitably defined boundary value problems that we omit for brevity, and are given in detail in Refs. [21] and [13], as are the exact expressions for $U(x,\theta)$ and $V(x,\theta)$.

1. Small eccentricity

In Fig. 4(a) we show the flexion field magnitude for the eccentric Taylor vortex for the case of $\epsilon=0.1$, $\delta=0.096$, and $A=1000$, in accordance with the values chosen in Ref. [13]. In Fig. 4(b) the local Reynolds number is shown, validating as in the case of the concentric flow, that the center of the vortex can be considered as inviscid. More illuminating is a plot of the Eulerian diagnostic $\mathcal{D}$ which ''measures'' the interaction of the geometric and the dynamical symmetry. This is shown in Fig. 5(a) (for $\theta=-\pi/2$) and two sections of this surface with the planes $z=0.5$ and $z=1.5$ are shown in Figs. 5(b) and 5(c), respectively.

It is interesting to compare Figs. 5(b) and 5(c) with the surface of section $\theta=0$ for the particle paths in Fig. 6. It is clearly seen that regions where $\mathcal{D}$ deviates from zero highlight the chaotic region. The section of $\mathcal{D}$ with the $z=0.5$ plane highlights a single chaotic region, and the section of $\mathcal{D}$ with the $z=1.5$ plane highlights two chaotic regions – both in accordance with what is observed in the surface of section. Because of the remnants of the rotational symmetry near the walls, the diagnostic $\mathcal{D}$ is small there. Comparison with Fig. 6 (also see Fig. 3(d) in Ref. [13]) shows that chaotic orbits indeed stay away from the cylinders.

Note that we correlated $\mathcal{D}$ at $\theta=-\pi/2$ with the surface of section at $\theta=0$. We did this because there is a ''memory effect.'' That is, a particle's motion observed at some angular position is determined by events upstream of it. That is, the diagnostic varies with θ (and hence so do the flexion field and the local Reynolds number). In the case of the wavy vortex the diagnostic is similar for different ψ, so the memory effect is not that apparent.

2. Large eccentricity

We now consider the case of large eccentricity with $\epsilon=0.5$, $\delta=0.096$, and $A=100$. The position of the widest gap between the cylinders is $\theta=0$. At this eccentricity there is a zone of recirculation in the wide gap region of the system. At $\theta=0$ it extends from about $x=0$ to $x=0.5$. (See Ref. [13] for further details.)

Since the large eccentricity case is further away from the rotationally symmetric Couette flow, we choose not to include the measure of rotational symmetry in the diagnostic. Thus here we define $\mathcal{D}$ by

$$\mathcal{D}=(\nabla\times\boldsymbol{\omega})^2\left(\frac{\partial\mathbf{v}}{\partial z}\right)^2. \tag{3.12}$$

In Fig. 7 we show the flexion field magnitude and the local Reynolds number, and in Fig. 8 the diagnostic at $\theta=-\pi/2$ for the large eccentricity Taylor vortex. Inspection of Fig. 8 shows that remnants of the symmetries are still present in the region close to $x=-0.2$, which corresponds in Fig. 9 to the center of the vortex where the orbits are regular. The symmetries are broken near the inner wall and near the middle of the annulus at $x\simeq 0$.

We now compare Fig. 8 with the surface of section Fig. 9 obtained at the downstream location $\theta=0$. Inspection of Fig. 8 shows that remnants of the symmetries are still present in the region close to $x=-0.2$, which corresponds in Fig. 9 to the center of the vortex where the orbits are regular. The symmetries are broken near the inner wall and in the outer half of the annulus ($0\leqslant x\leqslant 1/2$). Near the inner wall the symmetry is broken only weakly, and this correlates with the fact that the dynamics are more regular near the inner wall. The stronger symmetry breaking in the outer half of the annulus corresponds to orbits (originating from that part of the annulus at $\theta=-\pi/2$) passing near or through the broken ''dividing'' stream surface into the recirculation region where the dynamics get ''reshuffled.'' This is the primary source of stochasticity in this flow.

We also find that, at least in these examples, the spatial gradients of $\mathcal{D}$ increase with A. Ashwin and King found that the area occupied by the regular orbits decreased with an increase in A. Thus it is tempting to conjecture that a relationship exists between the area occupied by the regular trajectories and the spatial gradients of $\mathcal{D}$. However, a definite statement must await further development of the theory and further numerical studies.

IV. TIME-DEPENDENT CASE

A desirable extension of the methods presented here would be to the case of flows that are essentially unsteady, in the sense that they cannot be made steady by a transformation to a moving frame. Unfortunately, the dynamical symmetry, provided by Arnold's theorem in the steady case, ceases to provide integrability in this case. Still, something can be done when a spatial volume-preserving symmetry is present. An example is provided by the case of translational or rotational symmetry of a Euler flow. The spatial symmetry provides a stream function for the flow, and the velocity field is given by

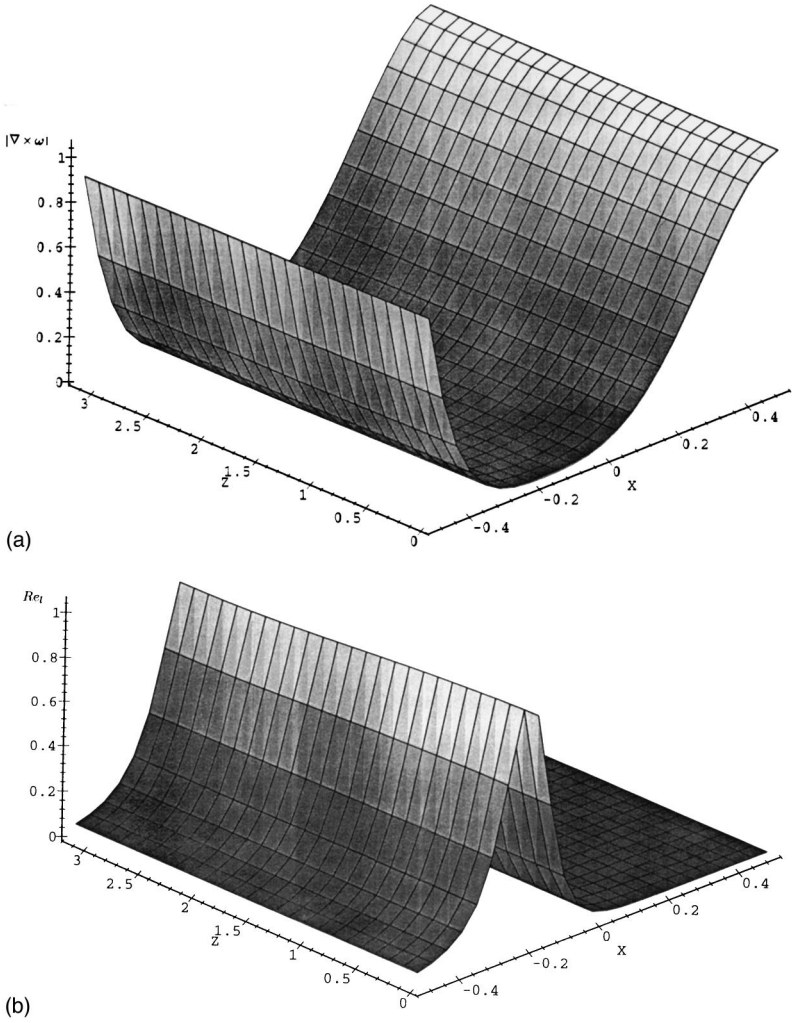

FIG. 7. (a) The flexion field magnitude $|\nabla \times \boldsymbol{\omega}|$, and (b) the local Reynolds number Re_l for the large eccentricity ($\epsilon = 0.5$) Taylor vortex case. The vortex amplitude is $A = 100$. The quantities are calculated at $\theta = -\pi/2$, and are scaled by their maximum value there. The outflow boundary is located at $z = 0$, and the inflow boundary at $z = \pi$.

$$\dot{x} = \frac{\partial \psi(x,y,t)}{\partial y}, \quad \dot{y} = -\frac{\partial \psi(x,y,t)}{\partial x}, \quad \dot{z} = f(x,y,t) \tag{4.1}$$

(see Refs. [11,24]). In the case of translational symmetry, it is easy to see that the equation for the magnitude of the vorticity ω_z in the direction z of the symmetry is

$$\frac{\partial \omega_z}{\partial t} + \mathbf{v} \cdot \nabla \omega_z = 0. \tag{4.2}$$

It was shown in Ref. [24] that this conservation law is associated with a dynamical symmetry generated by the spatial gradients of the vorticity. Now assume that the dependence on the time of the flow is periodic. Then ω_z is a constant of motion for $\mathbf{v}(x,y,t)$. The corresponding Navier-Stokes flow is given by

$$\frac{\partial \omega_z}{\partial t} + \mathbf{v} \cdot \nabla \omega_z = \nu \triangle \omega_z . \tag{4.3}$$

The diagnostic for nonintegrability needs to be constructed

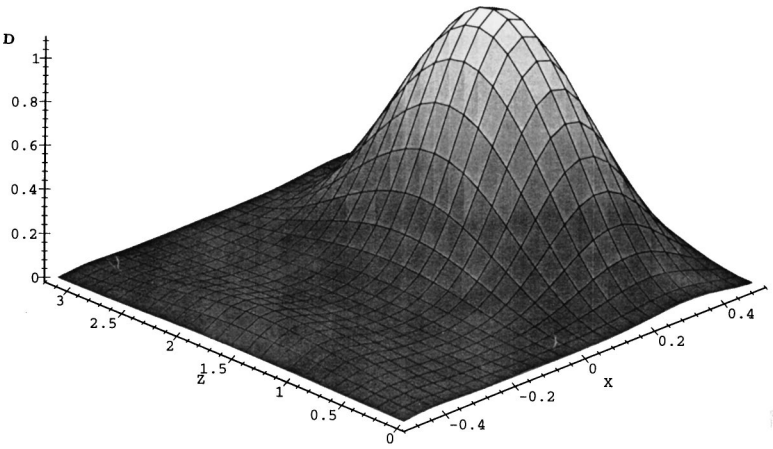

FIG. 8. The Eulerian diagnostic $\mathcal{D}$ at $\theta = -\pi/2$, scaled by its maximum value for the large eccentricity Taylor vortex case.

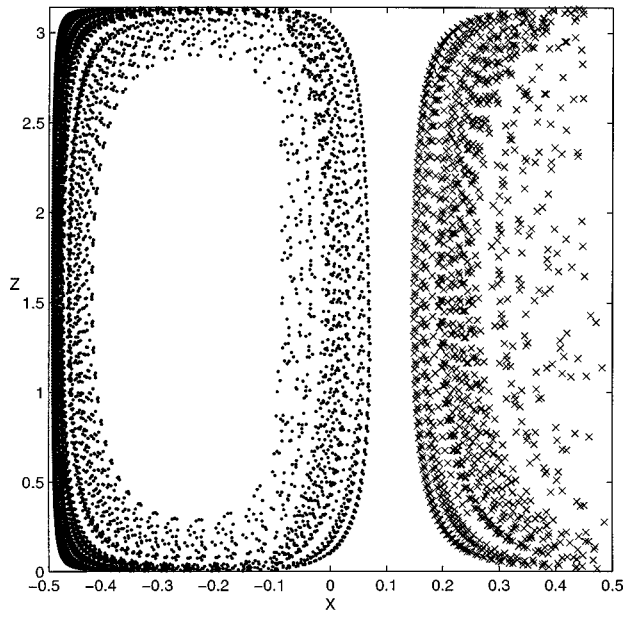

FIG. 9. Surface of section for the large eccentricity Taylor vortex taken at the position of largest gap ($\theta=0$). The vortex amplitude is $A=100$. At $\theta=0$ the recirculation zone extends from about $x=0$ to the outer cylinder at $x=\frac{1}{2}$. Note that all intersections of the orbit with the surface are shown. The dots indicate intersections of the orbit traveling in the same direction as the inner cylinder, and the crosses mark the intersections in the opposite direction. When the orbit is in the recirculation zone, intersections in both directions often occur.

differently than was done in the steady case, since the absence of either symmetry (geometrical, translational symmetry, or dynamical Euler symmetry) is enough to render the flow nonintegrable. Thus one possible diagnostic is

$$\mathcal{D}=|\triangle\omega_z|+\left|\frac{\partial\mathbf{v}}{\partial z}\right|+\left|\frac{\partial\mathbf{v}}{\partial\theta}\right|. \tag{4.4}$$

A similar treatment can be done in the case of quasigeostrophic flows for which the potential vorticity $q(x,y,t)=\triangle\psi+\beta y$ is the conserved quantity.

Another example of an essentially time-dependent flow with remnants of spatial symmetry, suitable for the perturbative methods described here, is that of modulated wavy vortex flow. We will pursue further investigation of the time-dependent case in future work.

V. DISCUSSION AND CONCLUSIONS

In this paper, based on symmetry considerations, we introduced Eulerian diagnostics that serve as an indicator for determining regions where chaotic streamlines may appear in three-dimensional steady Navier-Stokes flows. Diagnostics are tested on two approximate analytical solutions of the Navier-Stokes equation. A good correlation is found to exist between the proposed diagnostic and the particle orbits. Unfortunately, the analytic solutions we used are the only ones available to us. For a more exhaustive test of our diagnostic tools we need numerical solutions or experimental measurements. The diagnostic tools presented here can highlight the location of chaotic particle paths without the need to integrate particle orbits in a large class of flows.

It is a built-in assumption of this paper that the flows we study are such that velocity and vorticity vectors are at an angle that is an order of magnitude larger than the inverse Reynolds number. We do not know of any experimental examples in which this would be violated. In case such a situation exists, and velocity is uniformly represented as vorticity multiplied by a constant, ABC flows would provide a good model. In the case of a more general Beltrami flow, the same type of diagnostic as presented in this paper can be derived.

ACKNOWLEDGMENTS

We wish to thank the EPSRC under the Nonlinear Initiative, and NATO for financial support. We also wish to thank Dr. P. Ashwin for his invaluable advice and interest.

[1] H. Aref, J. Fluid Mech. **143**, 1 (1984).
[2] J. Ottino, *The Kinematics of Mixing: Stretching, Chaos and Transport* (Cambridge University Press, Cambridge, 1989).
[3] S. Wiggins, *Chaotic Transport in Dynamical Systems* (Springer-Verlag, New York, 1992).
[4] M. Feingold, L. P. Kadanoff, and O. Piro, J. Stat. Phys. **50**, 529 (1988).
[5] K. Bajer and H. Moffatt, J. Fluid Mech. **212**, 337 (1990).
[6] H. A. Stone, A. Nadim, and S. Strogatz, J. Fluid Mech. **232**, 629 (1991).
[7] D. D. Holm and Y. Kimura, Phys. Fluids A **3**, 1033 (1991).
[8] R. S. MacKay, J. Nonlinear Sci. **4**, 329 (1993).
[9] S. W. Jones and W. R. Young, J. Fluid Mech. **280**, 149 (1994).
[10] I. Mezić, Ph.D. thesis, California Institute of Technology, 1994.
[11] I. Mezić and S. Wiggins, J. Nonlinear Sci. **4**, 157 (1994).
[12] I. Mezić, A. Leonard, and S. Wiggins, Physica D (to be published).
[13] P. Ashwin and G. P. King, J. Fluid Mech. **285**, 215 (1995).
[14] P. Ashwin, G. W. Mann, and G. P. King, Phys. Rev. Lett. **75**, 4610 (1995).
[15] P. Ashwin and G. P. King, J. Fluid Mech. **338**, 341 (1997).
[16] V. I. Arnold, Ann. Inst. Fourier **16**, 316 (1966).
[17] C. Truesdell, *The Kinematics of Vorticity* (Indiana University Press, Bloomington, IN, 1954).
[18] V. V. Kozlov, Russ. J. Math. Phys. **1**, 57 (1993).
[19] G. Sposito, Int. J. Eng. Sci. **35**, 197 (1997).
[20] A. Davey, R. DiPrima, and J. Stuart, J. Fluid Mech. **31**, 17 (1968).
[21] R. DiPrima and J. Stuart, J. Fluid Mech. **67**, 85 (1975).
[22] V. I. Arnold, *Mathematical Methods of Classical Mechanics* (Springer-Verlag, New York, 1978).
[23] T. Dombre *et al.*, J. Fluid Mech. **167**, 353 (1986).
[24] G. Haller and I. Mezić, Nonlinearity (to be published).